2017 IEEE International Conference on Robotics and Automation (ICRA)
Singapore, May 29 - June 3, 2017

On the Impact Force of Human-Robot Interaction: Joint Compliance vs. Link Compliance

Yu She, *Student Member, IEEE*, Deshan Meng, Junxiao Cui and Hai-Jun Su, *Member, IEEE*

Abstract— **In this paper, we study the effect of mechanical compliance on the impact force of human-robot interactions, more specifically the maximum impact force during a collision. Here we consider two methods of introducing compliance to industrial manipulators: joint compliance and link compliance. To compare their effect on the maximum impact force, we study two designs of a 2D robot link: a rigid link with torsion spring at the joint and a uniform compliant link. The dynamic impact model is based on the Hertz contact model. The results show that the compliant joint solution could produce a larger impact force than that of the compliant link solution if the arm mass is larger than that of the end mass, given the same lateral stiffness and all other inertial parameters (e.g. mass). Simulations and experiment have been done and verified this conclusion. The research demonstrates that the compliant link solution could be a promising approach for addressing safety concerns of human robot interactions.**

I. Introduction

In recent years, there has been growing interests in collaborative robots or simply co-robots. Unlike conventional industrial robots which are kept separated from operators, co-robot [1] is designed to physically interact with humans in a shared workspace. The safety becomes a prominent consideration for co-robots.

Intentionally introducing compliance to the mechanical design (either joints or links) can increase safety when an impact occurs during a human-robot interaction. Many studies have been done on the joint compliance, while relatively less research works on the link compliance to the safety contribution for human robot interaction. Especially, the question of when we should use joint compliance or link compliance is yet to be answered.

Germany Aerospace Center employed compliant joints for their anthropomorphic hand arm system [2]. The solution consists of a floating spring and two superimposed cam mechanisms. Interdepartmental Research Center "E. Piaggio" studied the design, prototype, and control of the variable impedance actuation (VIA) and variable stiffness actuators (VSA)[3], [4]. The VSA I [4] is realized by stretching and releasing a timing transmission belt, which enable the stiffness of the actuator vary rapidly and continuously. The VSA II [3] is designed based on four bar mechanisms with nonlinear torque displacement characteristic. More researches on VSA could be found but not limit to [5], [6].

Research on compliant links for human-robot application is relatively less explored. Park et al. [7] developed a safe link mechanism. The link has a high stiffness if the external force is lower than a critical threshold but could abruptly drop down if the force exceeds a threshold. Lopez-Martinez et al. [8] and Zhang et al. [9] studied similar switch off mechanisms on flexible linkage to ensure safety for human robot interaction. She et al. [10] presented the design of a tunable stiffness robotic link, which showed a 40% impact force reduction comparing the stiff and compliant states of the link.

Since both joint compliance and link compliance solutions can enhance safety level for human robot interactions, it is necessary to compare their performance in order to guide the mechanical design process. Even though head impact criterion (HIC) is the most widely used criterion to evaluate severity of collision in a human robot interaction, there are some confusions and ambiguities of HIC in literatures [11]. Impact force is an alternative criterion to evaluate severity and recommended by some researchers [12]. In this article we will try to evaluate the performance of these two solutions based on the maximum impact force.

We start this paper with problem and goal statement in section 2. In section 3, the contact force model is presented, and compression tests are conducted to determine the parameters of the contact model. Calculation of the maximum impact force is presented in section 4. In section 5, simulation and analysis are studied regarding to the effect of mass and stiffness on the impact force. Experimental verification is conducted in section 6. Finally, conclusions and future work are presented in Section 7.

II. Problem and Goal Statement

Prior to the study of the impact force model, let us define some parameters and define our goal. Fig. 1(a) shows a typical rigid link with a torsion spring at the joint, while Fig. 1(b) shows a typical revolute joint and a uniform compliant link. To compare the impact results of these two systems, we assume they have the same length (L), mass (m) and rotational inertia (J), and payload (m_e).

We also assume both designs have the same lateral stiffness at the free end. The lateral stiffness of the CJ design in

Yu She is a Graduate Research Associate of Dept. of Mechanical and Aerospace Engineering, The Ohio State University, Columbus, OH 43210, USA she.22@osu.edu

Deshan Meng is a Graduate Student of Dept. of Mechanical and Automation, Harbin Institute of Technology Shenzhen Graduate School, Guangdong, Shenzhen 518055, P.R. China dsmeng@hit.edu.cn

Junxiao Cui is a Master Student of Dept. of Mechanical and Aerospace Engineering, The Ohio State University, Columbus, OH 43210, USA cui.373@buckeyemail.osu.edu

Hai-Jun Su is an Associate Professor of Dept. of Mechanical and Aerospace Engineering, The Ohio State University, Columbus, OH 43210, USA su.298@osu.edu. Corresponding author.

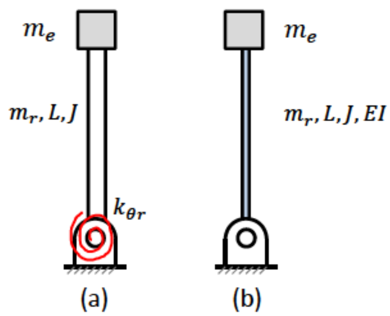

Fig. 1: (a) A rigid link with a compliant joint (CJ) at the root, (b) a revolute joint with a uniform compliant link (CL). Both designs have the same length (L), mass (m_r) and rotational inertia (J), and payload (m_e).

Fig. 1(a) is calculated as

$$k_\delta = \frac{k_{\theta r}}{L^2} \tag{1}$$

And the lateral stiffness of the uniform CL in Fig. 1(b) is calculated by

$$k_\delta = \frac{3EI}{L^3} \tag{2}$$

Equating (1) and (2) leads to the torsional stiffness of the CJ,

$$k_{\theta r} = \frac{3EI}{L} \tag{3}$$

When an unexpected impact occurs at the free end, our goal is to compare the maximum impact force to a human head of the same mass for these two designs.

III. Contact Force Model

Before we develop the model to compute the impact force, we must first characterize the surface contact force between a human operator and a robot arm.

A. The Hertz Model

In this paper, we mimic the impact of human's forehead with a robot arm. As shown in Fig. 2, a hard base and soft cushion material, representing the bone and skin of human respectively, are used to simulate the human's forehead. A hard spherical dome is used to simulate the contact region of a robot arm. Given a compression force f from the dome, an indention of δ_c will be generated on the soft surface.

The contact force can be calculated by the Hertz contact law

$$f = k_c \delta_c^n \tag{4}$$

where k_c and n are the contact surface stiffness and Hertz exponent respectively. They are determined by material and geometry properties of the local contact region. δ_c is the indention or penetration.

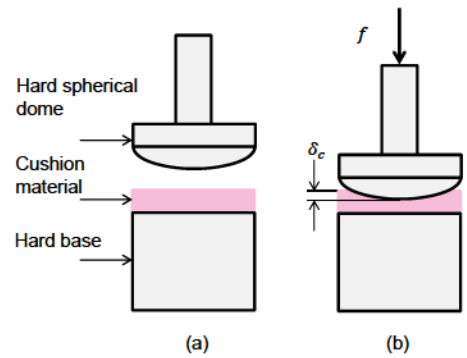

Fig. 2: The schematic of Hertz surface contact model: (a) the hard spherical dome simulates a robot arm, the hard base and soft cushion material representing bone and skin of human forehead, (b) the dome is against the cushion material by a compression force f and induces an indention δ_c.

B. Compression Test

To obtain the parameters of the Hertz model, we conducted compression tests for different samples, as shown in Fig. 3. A aluminum dome with a radius of 71.5 mm is machined to represent the contact area of a robot. Different samples with a wide range of mass were tested. Samples are acrylonitrile butadiene styrene (ABS) block, aluminum block, and iron block weighing 39 g, 398 g, 4008 g, representing relatively light weight, medium weight, and heavy weight, respectively.

To simulate the impact between a robot and human, a soft material is fabricated using Shape Deposition Manufacturing (SDM) [13] and attached on the blocks servicing as the skin. The properties of the soft layer refers that of the human skin. Silicon Max 20 (Shore A Hardness is 20A) is the material used to mimic the human skin. When the blocks and aluminum dome are ready, the static test is conducted by a Mark-10 compression system.

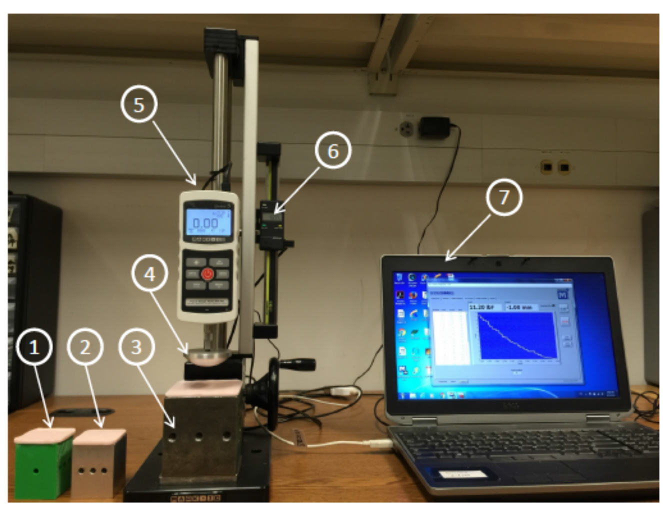

Fig. 3: Parameters specification of contact model via static test. 1 ABS block sample, 2 Aluminum block sample, 3 Iron block sample, 4 Aluminum dome, 5 Force sensor, 6 Travel display, 7 Laptop collecting data.

As shown in Fig. 3, the skinned block is placed on the platform of the Mark-10 system (ES30, 1000 N), and the aluminum dome is installed on the force sensor (M5-100, 500×0.1 N). A hand wheel can be operated to control the motion of the force sensor, hence the compression between the dome and skinned block. A travel display (ESM001, 150×0.01 mm) is used to monitor the indention of the test. A laptop is able to collect the data from the sensor.

The test results are shown in Fig. 4. Fitting curves are plotted to find the parameters of the contact model. We found $k = 7.359 \times 10^7$ N/m and $n = 1.961$ for skinned aluminum block, $k = 9.642 \times 10^7$ N/m and $n = 2.002$ for skinned iron block, and $k = 1.311 \times 10^7$ N/m and $n = 1.817$ for skinned ABS block, respectively.

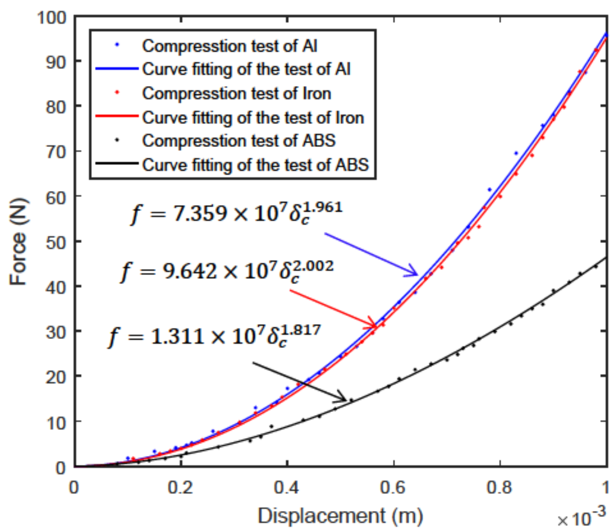

Fig. 4: Curve fitting the Hertz contact force model with the compression test data.

IV. Calculation of Maximum Impact Force

Suppose an unexpected impact occurs between a typical compliant robotic link and an operator as shown in Fig. 5(a). The robot link has a mass of m_r, length of L, and rotational inertia J, carrying an end mass m_e. Driven by a torque controller $\tau(t)$, the link hits the human operator with a mass m_h at an angular velocity $\omega(t)$, and the contact stiffness of the impact is k_c.

To study the effect of link compliance on the impact force, we employ its Pseudo-Rigid-Body (PRB) model [14] which approximate the tip deflection with two rigid segments joined by a torsion spring $k_{\theta p}$ as shown in Fig. 5(b). It is well known that the position of this torsional spring is given by the so-called characteristic radius (γ) from the tip of the link ($\gamma = 2/3$ for a small deflection [15], $\gamma = 0.85$ for a large deflection). The torsional stiffness of the PRB model is $k_{\theta p} = \pi E I \gamma^2 / L$ [14].

If the compliant link is simplified into a PRB model, the impact system can now be described as a link-spring-mass system, as shown in Fig. 5(b). A simplified mass-spring-mass model, as shown in Fig. 5(c), has been proposed in [16], where m_{eff} is the effective mass of the robot and end mass, and k_o is the overall stiffness of the impact. The overall stiffness is contributed by the serial connection of the lateral stiffness of the compliant link and contact stiffness of the impact, as shown in Fig. 5(d).

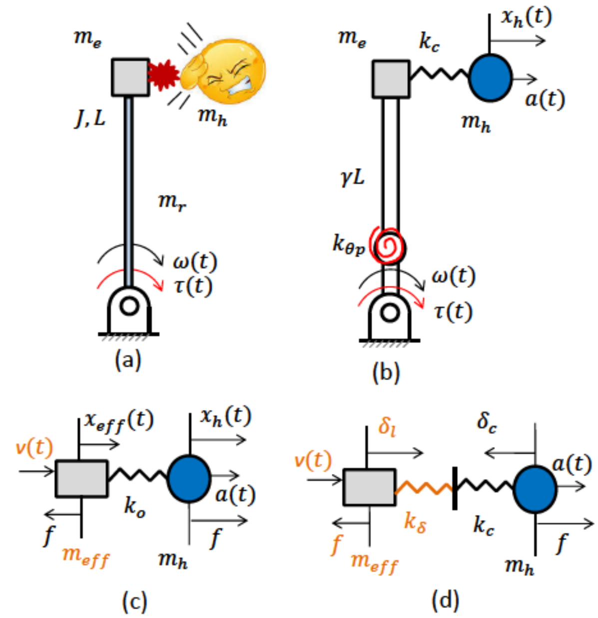

Fig. 5: (a) A typical impact between a compliant robot link and an operator, (b) the corresponding link-spring-mass model, (c) the mass-spring-mass model with an equivalent spring k_o, (d) the mass-spring-mass model with two serially connected springs.

By using the kinetic energy of the robot arm and the end mass, we can calculate their effective mass as

$$m_{eff} = m_e + \frac{1}{3}\gamma m_r \tag{5}$$

And the surface indention can be calculated from Hertz contact force model (4) as

$$\delta_c = \sqrt[n]{\frac{f}{k_c}} \tag{6}$$

The lateral deflection of the free end is calculated by

$$\delta_l = \frac{f}{k_\delta} \tag{7}$$

The overall displacement of the free end is the sum of the indention of the contact surface and lateral deflection of the link,

$$\delta = \delta_l + \delta_c \tag{8}$$

The overall stiffness for Fig. 5(d) can be represented by

$$k_o = \frac{f}{\delta} = \frac{f k_\delta}{f + k_\delta \sqrt[n]{f/k_c}} \tag{9}$$

Eq. (9) shows that the overall stiffness is highly nonlinear and depends on the impact force f.

Assume the displacement of the effective mass and the human operator could be represented as $x_{eff}(t)$ and $x_h(t)$ respectively. According to Newton second law, we have

$$m_{eff}\ddot{x}_{eff}(t) = -f(t) \tag{10}$$

$$m_h \ddot{x}_h(t) = f(t) \tag{11}$$

The overall displacement of the free end can be described as

$$\delta(t) = x_{eff}(t) - x_h(t) \tag{12}$$

For a given value of n and initial conditions $\delta(0) = 0, \dot{\delta}(0) = v_0$, one may numerically solve the ordinary differential equations Eqs. (4, 10, 11, 12) to obtain the dynamics response of both robot and human head. Here we will seek to derive analytical results for the special case of $n = 1$.

When the contact surface has a linear stiffness, the overall stiffness (9) can be simplified into

$$k_o = \frac{k_c k_\delta}{k_c + k_\delta}$$

It is not hard to analytically solve Eqs. (4, 10, 11, 12). The maximum impact force occurs at the instant of maximum compression when the velocity $\dot{\delta} = 0$

$$f_{max} = v_0 \sqrt{k_o \frac{m_h m_{eff}}{m_h + m_{eff}}} \tag{13}$$

where v_0 is the initial impact velocity. Note this result agrees with the one based on energy method [17].

V. Effect of Mass and Stiffness on Impact Force

Let us first study effect of mass on the maximum impact force for the linear contact force model, i.e. $n = 1$. Substituting (5) into (13) yields

$$f_{max}(\gamma) = v_0 \sqrt{k_o \frac{m_h(m_e + \gamma m_r/3)}{m_h + m_e + \gamma m_r/3}}. \tag{14}$$

By observing Eq. (14), we can make some conclusions regarding to the effect of γ may lower the impact force:

1) if the mass of pay load is much heavier than the mass of robot itself, i.e. $m_e \gg m_r$, the impact force is dominated by the pay load. Therefore, the effect of γ on f_{max} is limited. In other words, neither CL design nor CJ design have much effect on the maximum impact force.
2) otherwise, the effect of γ will affect f_{max} to a certain degree. And the smaller the value of γ, the smaller the maximum impact force. In other words, CL designs have extra benefits over CJ design in terms of reduced impact force.

However for nonlinear case $n \neq 1$, it is not obvious to see this effect as no explicit formulation is available. For this case, we numerically solve the impact dynamics equations. In particular, we are interested in the case of $n = 2$ as our experimental data of materials we used shows the Hertz model is very close quadratic.

Now let us study effect of mass and material stiffness on the impact force. To minimize the simulations, we set the mass of robot $m_r = 10$ kg, stiffness of contact surface $k_c = 1 \times 10^8$ N/m, and the initial impact velocity $v_0 = 2$ m/s to be constant. A typical value of human head is 4 kg in literature of human-robot interaction [11]. We study two

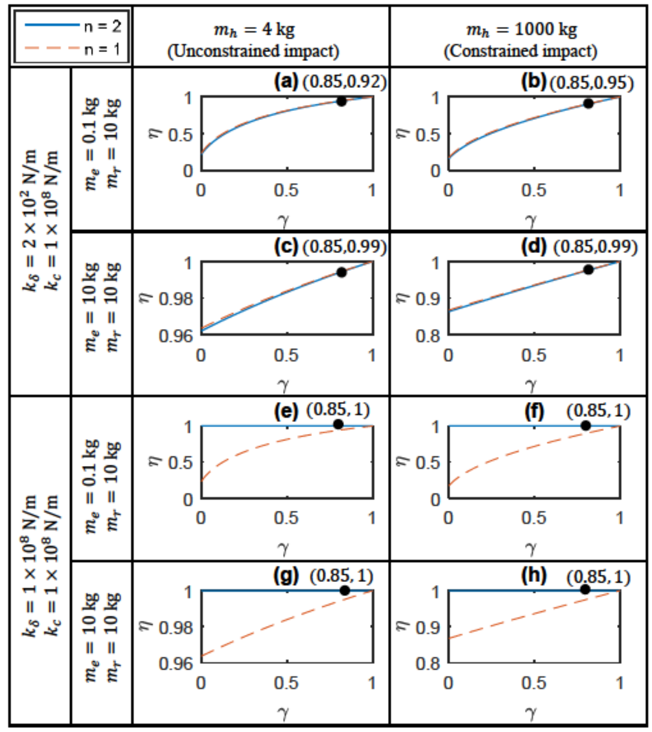

Fig. 6: The maximum impact force ration η vs. γ for all eight design cases. The blue solid lines represent the nonlinear Hertz model $n = 2$ and the orange dashed lines are for the linear contact force model $n = 1$.

cases of mass of human head $m_h = 4$ kg and $m_h = 1000$ kg, where simulate unconstrained impact and constrained impact (against the wall) respectively. With regard to stiffness of CL, we also study two cases: rigid link ($k_\delta = 1 \times 10^8$ N/m) and compliant link ($k_\delta = 2 \times 10^2$ N/m). Furthermore, we study two cases for pay load: light load $m_e = 0.1$ kg and heavy load $m_e = 10$ kg. Enumerating the two cases for each of these three parameters m_h, k_c and m_e, we obtain eight design combinations which are shown in Fig. 6. For each case, we study the effect of γ on the maximum impact force. In particular, we exam the ratio of the maximum impact for the CL γ over that for CJ $\gamma = 1$, i.e.

$$\eta = \frac{f_{max}(\gamma)}{f_{max}(1)}. \tag{15}$$

The result of the numerical simulation is shown in Fig. 6. This figure shows the increase rate of the impact force along with the increase of the γ value. The blue solid line is plotted based on the nonlinear Hertz model of $n = 2$, while the orange dashed line shows the linear force model with $n = 1$. For each figure, we also mark the value of η at $\gamma = 2/3$ i.e. uniform compliant link.

From Fig. 6, we conclude that the CL solution has benefits of reducing the maximum impact force over the CJ solution if the mass of payload m_e is much smaller than the robot mass m_r. More specifically $\eta = 0.89$ for unconstrained impact and $\eta = 0.82$ for constrained impact.

VI. Experimental Verification

A. The experiment principle

Recall our goal is to compare the effect of link compliance and joint compliance on the maximum impact force. To have a fair comparison, both designs must have the same mass, link length, lateral stiffness and rotational inertia. To ensure this, we employ a single flat beam of length L with a large ratio of width (w) over thickness (t). It is well known that a 2D beam has a high stiffness in the beam plane and a low stiffness in the out-of-plane direction. In the CJ design shown in Fig. 7(a), the impact direction is in the beam plane. A torsion spring is connected between the motor shaft and the beam. The stiffness of the torsion spring $k_{\theta r}$ is determined by the equal lateral stiffness requirement, i.e. Eq. (3). While in the CL design, the impact direction is perpendicular to the beam plane. The beam is rigidly attached to the motor shaft. Note when the $w/t = 25$, we have a change in lateral stiffness as high as 625 times.

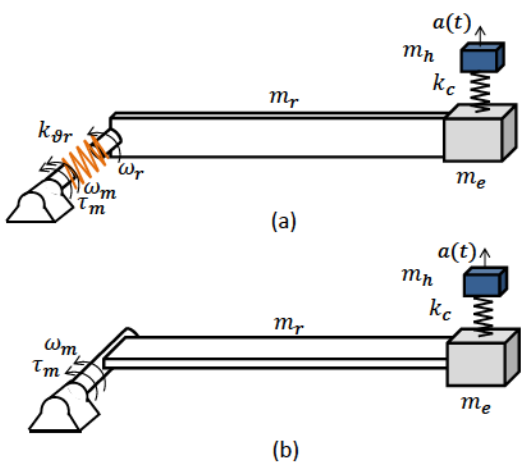

Fig. 7: (a) The compliant joint design and (b) the compliant link design have identical mass, length, rotational inertia and lateral stiffness.

B. Hardware design

The setup of the impact experiment is shown in Fig. 8. The compliant link to be tested is labeled '5', carrying a load at the tip. The operator is modeled by another link with a concentrated mass at the tip, as labeled '4' in this figure. Instead of controlling the robot link to hit the operator, we set up the operator to hit the robot link, due to the torsion spring installed on the axis of the robot link. We assume that the switching of the roles does not affect our evaluation of the impact force. The frame of the CL is fixed while the frame of the operator link is adjustable in x, y, and z direction. The fixed frame is able to switch the configuration of the compliant robot link from CJ design to CL design.

The part mimicking human operator can be lifted up and released at a certain angle, then obtain a specific desired impact velocity. The rotation speed is monitored by an encoder. A pointer with a gridded disk are assist in order to ensuring repeatability of the tests. Numerous testings of lifting and releasing the operator link at a certain angle

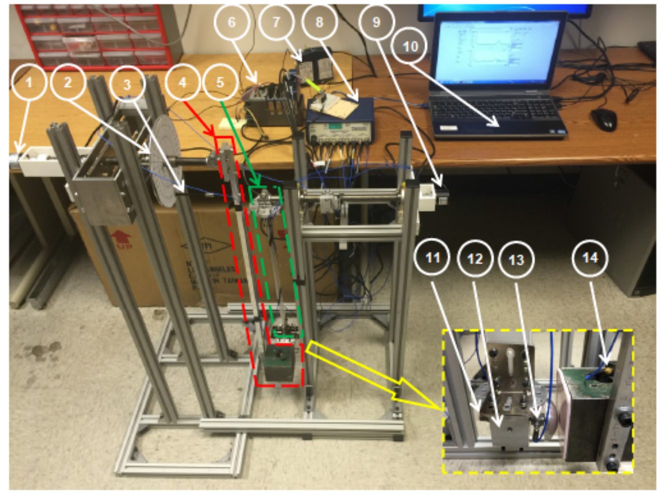

Fig. 8: The experiment setup of impact test: 1. Encoder on the operator side, 2. Labeled disk, 3. Pointer, 4. Link on the operator side, 5. Link on the robot side, 6. NI controller, 7. Power supply, 8. Signal conditioner, 9. Encoder on the robot side, 10. Laptop, 11. Acceleration sensor on the robot side, 12. Payload, 13. Force sensor, 14. Acceleration sensor on the operator's side.

have been done and the results confirmed the repeatability. Acceleration sensors labeled '14' (PCB 356A15) and '11' (PCB 352C03) are installed on the operator block and load block respectively. A force sensor labeled '13' (PCB 208C04) is assembled between the load and the impactor dome. The sensor data are measured by a signal conditioner (PCB 482C05) and collected by a controller (NI cRIO-9014).

With this experiment setup, extensive tests have been done to verify the assumptions. We first selected a CL made of polypropylene. Based on the rough dimensions of the CL, we could find the range of the torsion spring stiffness. Then we specified a torsion spring with a stiffness of $k_{\theta r} = 1.2334$ Nm/rad. The dimension of the CL could be finalized based on the torsion spring. The CL weighs m_r = 51 g. The mass of the load is m_e = 412 g. The skinned aluminum block and iron block presented previously are used here for impact test. In this test, it is true that $m_e \gg m_r$, and the situation of the skinned aluminum block maybe regarded as the unconstrained impact, while skinned iron block as the constrained impact due to their weigh ratios.

The limitation of this test is that the compliant link is too light to find a sample of load to do the test under the condition of $m_r \gg m_e$. Therefore, a simulation platform was built in ADAMS to explore the effect of γ under this situation. All parts are build in Solidworks, which are the same as our actual test bed. Then they are exported to ADAMS with corresponding parameters, except the density of the load. It is worth noting the compliant beam is assigned the flexible attribute. The mass of load in this test could be a small value (here m_r = 0.1 kg). Then the impact simulations for CJ and CL designs are conducted and compared.

The experimental results are shown in Fig. 9 (a). Each test is repeated five times, and an average impact force with standard deviation in 95% confidence bounds are plotted. From the plot of the actual impact experiment, the CJ design performs slightly larger impact force than that of the CL design. It turns out that in these cases tuning γ cannot reduce the maximum impact force significantly. This is true for both the heavy operator ($m_h = 4008$ g) and light operator ($m_h = 398$ g). Therefore, the conclusion may hold for both constrained and unconstrained impact.

The ADAMS simulation results are shown in Fig. 9 (b). It is observed that the impact force of CJ design is larger than that of CL design. We may conclude the complaint link is safer than CJ for human robot interaction in terms of maximum impact force.

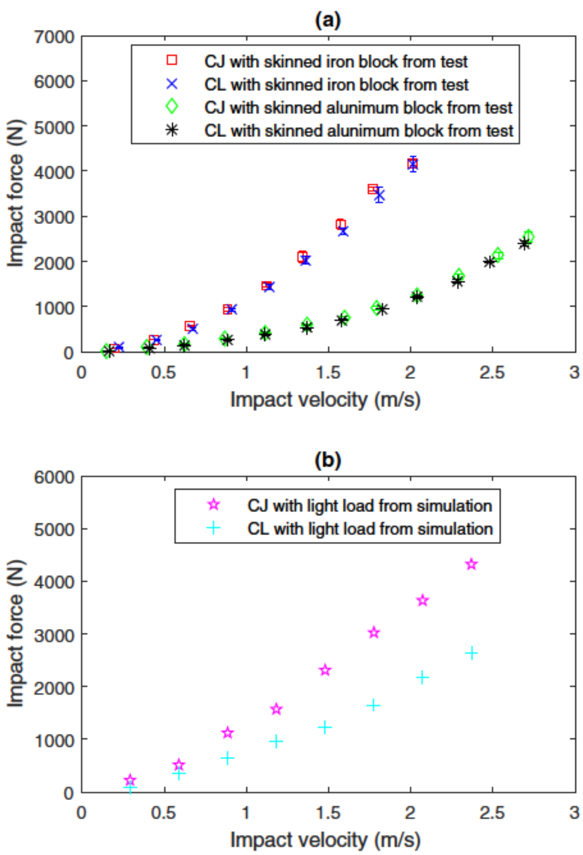

Fig. 9: (a) Physical impact tests of compliant joint (CJ) and compliant link (CL) designs, (b) impact simulation of CJ design and CL design considering a light load $m_e = 0.1$ kg.

VII. Conclusion and Future Work

This article studies the effect of link compliance and joint compliance on the impact force in human robot interactions. We first characterize the surface contact force model based on compression tests. We then derived the impact dynamics equations for calculating the maximum impact force. If the contact force model is linear, we obtained analytical expression of the maximum impact force in terms of mass and stiffness parameters. For nonlinear contact force model, we numerically solve the differential equations to determine the impact force. We then study how mass and stiffness affect the maximum impact force. By varying the mass of human head, stiffness of compliant link and mass of payload, we studied eight design cases by simulations and conclude that compliant link design may have a better performance over compliant joint designs when the robot mass is much larger than the end mass, given that the mass, link length, rotational inertia and later stiffness are all the same. We have also designed experiments to verify the simulations. Our preliminary results show that the trend agrees with the simulations for the light robot arm case. However due to limitation of availability of materials, we cannot carry out the experiments for the light load case (or heavy robot arm). Instead we conducted ADAMS simulations to verify our impact force model.

References

[1] Colgate, J. E., Edward, J., Peshkin, M. A., and Wannasuphoprasit, W., 1996. "Cobots: Robots for collaboration with human operators".

[2] Wolf, S., and Hirzinger, G. "A new variable stiffness design: Matching requirements of the next robot generation". In IEEE International Conference on Robotics and Automation, 2008. ICRA 2008, pp. 1741–1746.

[3] Schiavi, R., Grioli, G., Sen, S., and Bicchi, A. "VSA-II: a novel prototype of variable stiffness actuator for safe and performing robots interacting with humans". In IEEE International Conference on Robotics and Automation, 2008. ICRA 2008, pp. 2171–2176.

[4] Tonietti, G., Schiavi, R., and Bicchi, A. "Design and control of a variable stiffness actuator for safe and fast physical human/robot interaction". In Proceedings of the 2005 IEEE International Conference on Robotics and Automation, pp. 526–531.

[5] Zinn, M., Khatib, O., Roth, B., and Salisbury, J. K., 2004. "Playing it safe [human-friendly robots]". *IEEE Robotics & Automation Magazine*, ***11***(2), pp. 12–21.

[6] Pratt, G. A., and Williamson, M. M. "Series elastic actuators". In 1995 IEEE/RSJ International Conference on Intelligent Robots and Systems 95. 'Human Robot Interaction and Cooperative Robots', Proceedings, Vol. 1, pp. 399–406 vol.1.

[7] Park, J.-J., Kim, B.-S., Song, J.-B., and Kim, H.-S., 2008. "Safe link mechanism based on nonlinear stiffness for collision safety". *Mechanism and Machine Theory*, ***43***(10), pp. 1332–1348.

[8] Lpez-Martnez, J., Blanco-Claraco, J. L., Garca-Vallejo, D., and Gimnez-Fernndez, A. "Design and analysis of a flexible linkage for robot safe operation in collaborative scenarios". *Mechanism and Machine Theory*, ***92***, pp. 1–16.

[9] Zhang, M., Lalibert, T., and Gosselin, C. "Force capabilities of two-degree-of-freedom serial robots equipped with passive isotropic force limiters". *Journal of Mechanisms and Robotics*, ***8***(5), p. 051002.

[10] She, Y., Su, Hai-Jun Lai, C., and Meng, D. "Design and prototype of a tunable stiffness arm for safe human-robot interaction". In ASME 2016 International Design Engineering Technical Conferences and Computers and Information in Engineering Conference, American Society of Mechanical Engineers.

[11] Gao, D., and Wampler, C. W. "Head injury criterion". *IEEE Robotics Automation Magazine*, ***16***(4), pp. 71–74.

[12] Haddadin, S., Albu-Schäffer, A., and Hirzinger, G., 2007. "Approaching asimovs 1st law". In HRI Caught on Film, 2nd ACM/IEEE Int. Conf. on Human-Robot Interaction (HRI2007), Washington DC, USA, pp. 177–184.

[13] Cham, J. G., Bailey, S. A., Clark, J. E., Full, R. J., and Cutkosky, M. R., 2002. "Fast and robust: Hexapedal robots via shape deposition manufacturing". *The International Journal of Robotics Research*, ***21***(10-11), pp. 869–882.

[14] Howell, L. L., 2001. *Compliant mechanisms*. John Wiley & Sons.

[15] Su, H.-J., 2009. "A pseudorigid-body 3r model for determining large deflection of cantilever beams subject to tip loads". *Journal of Mechanisms and Robotics*, ***1***(2), p. 021008.

[16] Bicchi, A., and Tonietti, G., 2004. "Fast and soft-arm tactics". *Robotics & Automation Magazine IEEE*, ***11***(2), pp. 22–23.

[17] She, Y., Meng, D., Shi, H., and Su, H.-J., 2015. "Dynamic modeling of a 2d compliant link for safety evaluation in human-robot interactions". In Intelligent Robots and Systems (IROS), 2015 IEEE/RSJ International Conference on, IEEE, pp. 3759–3764.